A Study of the Fragmentation of cylindrical Shells of four Carbon Steels

Lars Eriksson
Division of Materials Research
Torkel Arvidsson
Division of Detonics

Research Institute of National Defence
Fack, S-10450 Stockholm 80

INTRODUCTION

The background of the studies presented here is our interest in understanding the fragmentation behaviour of High Explosive Shells. 20 years of experimental and theoretical work has given us a broad basis of data and semiempirical expressions. The work to be reported in this paper utilizes data from a recent fragmentation study by Johnsson (1972) and consists of a scanning electron microscope (SEM) study of the fragments from these experiments, completed by a structure investigation in a high voltage transmission electron microscope (HVEM).

In his report Johnsson (1972) has studied the fragmentation of cylindrical shell cases filled with high explosives. To enable a quantitative comparison between various shell case materials, the fragmentation number γ_o was determined, using the empirical relations (Hörner and Kemgren 1967)

$$M = M_o \exp(-\gamma m_1) \qquad (1)$$

where M_o is total weight of shell case in kg,

γ is a fragmentation number, dependent on geometrical dimensions, and

M is total weight of all fragments with weight $m \geq m_1$

and

$$\gamma = \gamma_o \exp(-26.4\,\phi - 15.8\,d/\phi) \qquad (2)$$

where ϕ is outer diameter and d thickness of shell case (dimension of both ϕ and d is meters; dimension of γ and γ_o is kg^{-1}).

Relation (1) is in good agreement with experimental data for $m_1 > 0.5 \cdot 10^{-3}$ kg.

γ_o depends on the properties of both the high explosive used and of the material in the shell case, but is independent of cylinder dimensions.

Among the shell case materials studied were three plain carbon steels containing approximately 0.6, 1.2 and 1.4 % C. The compositions and the corresponding fragmentation numbers are given in table 1 together with data subsequently obtained under identical experimental conditions for an Fe-0.16 % C steel. For reference, the composition of a material investigated by Beetle et al (1971) is also given in the table.

Table 1. Composition and fragmentation number γ_o of materials.

Nominal composition	C %	Si %	Mn %	P %	S %	Fragmentation number γ_o kg^{-1}
0.16 % C	0.16	0.23	0.71	0.009	0.023	$4.1 \cdot 10^3$
0.6 % C	0.57	0.56	0.81	0.020	0.020	$19.5 \cdot 10^3$
1.2 % C	1.17	0.59	0.72	0.021	0.022	$34.7 \cdot 10^3$
1.4 % C	1.36	0.66	0.74	0.020	0.020	$43.5 \cdot 10^3$
Beetle et al (1971)	0.51	0.81	1.63	0.012	0.021	-

It is clear from table 1 that the fragmentation number γ_o increases (which corresponds to increasing amounts of small fragments) with increasing carbon content in the small case material. It is also evident from an inspection of fragments of the various materials that a marked difference in fragment morphology exists between the low-carbon steel on one hand and all the other materials on the other hand. This is illustrated in figure 1, where typical sections through big fragments with an extension right through the original cylinder wall are shown. The plane of the sections is perpendicular to the original cylinder axis and the outer cylinder surface is to the left. Figure 1a shows a section through a fragment of the Fe-0.6 % C material, but is equally representative of the -1.2 and -1.4 % C materials. Fig 1b is from the Fe-0.16 % C steel. It can be seen that fragments of the Fe-0.6 % C steel (as well as of the Fe-1.2, and -1.4 % C materials) have both a radial surface adjacent to the outer surface and perpendicular to it (i.e. parallel to both the cylinder axis and one radius of the cylinder), and a shear surface adjacent

to the inner surface inclined at about 45 ° to it and parallel to the cylinder axis (notation according to Beetle et al 1971). The Fe-0.16 % C steel fragments have only shear surfaces. Since the four materials are compared under identical conditions of explosive loading, the differences in fracture behaviour between them must be due to variations in inherent material properties. The present investigation was undertaken in an attempt to find out whether the differences in fragmentation number reflect themselves in systematic differences in the appearance of the fracture surfaces of fragments of the high-carbon steels. Thus a study of these fracture surfaces in a JSM-U3 scanning electron

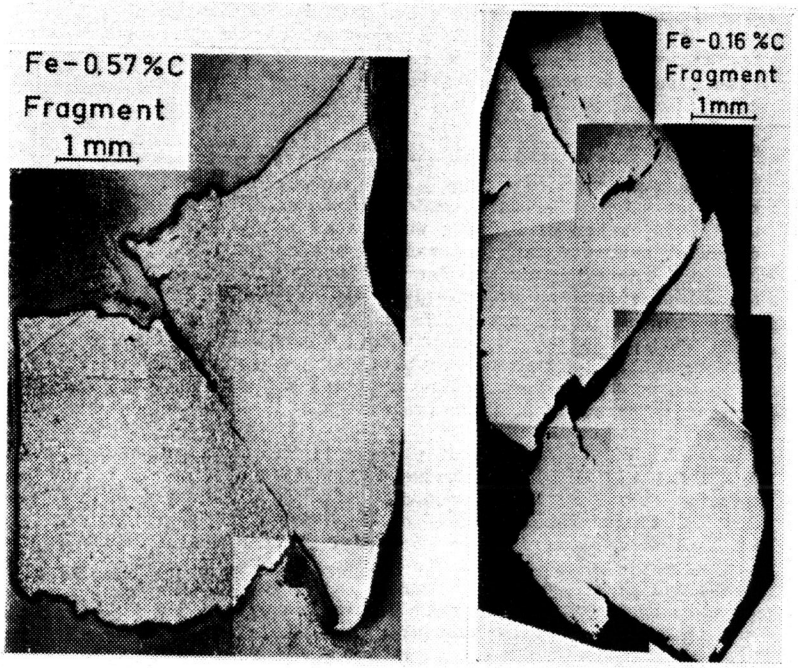

a b

Fig 1. Sections perpendicular to the original cylinder axis through fragment of (a) Fe-0.6 % C steel (nital etch), and (b) Fe-0.16 % C steel. The original outer cylinder surface is to the left.

microscope has been accomplished, as well as an investigation of the microstructures of the four materials in HVEM.

EXPERIMENTAL

1. Preparation of thin foil specimens

Steel tubes made of the various steel qualities were delivered in batches of 10 (except in the case of the Fe-0.16 % C steel, of which only one tube was investigated), and from these batches three tubes were selected for the fragmentation experiments, and from the same batches samples were taken for structure investigation.

Thin foil specimens suitable for transmission electron microscopy were prepared from slices which were polished mechanically and electrolytically in a mixture of chromic acid, acetic acid and distilled water, using a standard Bollman-technique. Thin foils were also prepared from fragments of the various materials. All these specimens were subsequently studied in a JEOL-JEM 1000 D transmission electron microscope, operating at 1 MeV.

2. Preparation of fragments for SEM study

The fragmentation experiments were accomplished in the following way. The steel tube which had an outer diameter of 0.075 m and a wall thickness of 0.009 m was placed in the center of a big circular concrete tank and was surrounded by a paper tupe of slightly larger diameter. The tank was filled with several m^3 of saw dust, which was prevented by the paper tube from direct contact with the steel tube. The fragments created at the explosion were thus recovered in the saw dust, and subsequent separation was accomplished by means of a big fan, which passed the mixture over a powerful magnet. Using this method, nearly 100 % of the fragments were found. Each fragment was then weighed and counted.

Since the SEM study was not planned until after Johnsson's work was finished, the fragments were stored some 3 months before preparation for SEM. This has led to some deterioration of the quality of the surfaces of most of the fragments due to incipient rust attack. The fragments were cleaned from the saw dust by repeated ultra-sonic rinsing in a copper-etylen-diamine (CED) solution. All of the fragments (except those made of the Fe-0.6 % C (steel) showed traces of rust attack. However, it was always possible to find areas virtually free from rust.

RESULTS

1. HVEM investigation

The structures of the four steel qualities (Fe-0.16, -0.6, -1.2 and -1.4 % C) in normalized condition are shown in fig 2 a-d. Grain diameters are approximately 23 μm, 10 μm, 7 μm and 7 μm respectively. The two hypoeutectoid steels show a structure of ferrite and pearlite, with characteristic spacings between cementite lamellae of roughly 0.1 μm and 0.2 μm respectively for Fe-0.16 and Fe-0.6 % C steel. The two high-carbon steels have mutually very similar structures. Their heat treatment was such as to produce a spheroidized structure, with cementite mainly occurring in globular form. Where cementite lamellae occur, their

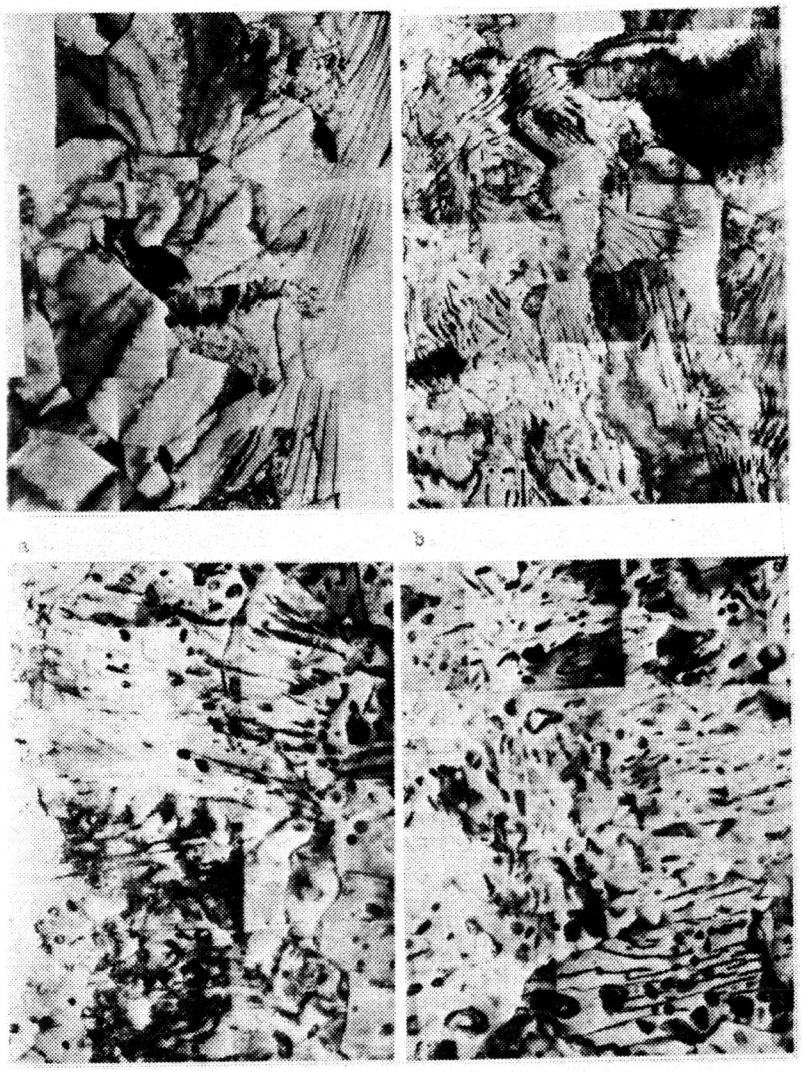

a b c d

Fig 2. Structure of normalized steels. (a) Fe-0.16 % C, (b) Fe-0.6 % C, (c) Fe-1.2 % C, (d) Fe-1.4 % C. HVEM

spacings are slightly larger than in the hypoeutectoid materials, about 0.5 μm in both Fe-1.2 and Fe-1.4 % C steel. Cementite both in the form of a film and in globular form is often observed in the grain boundaries of these materials.

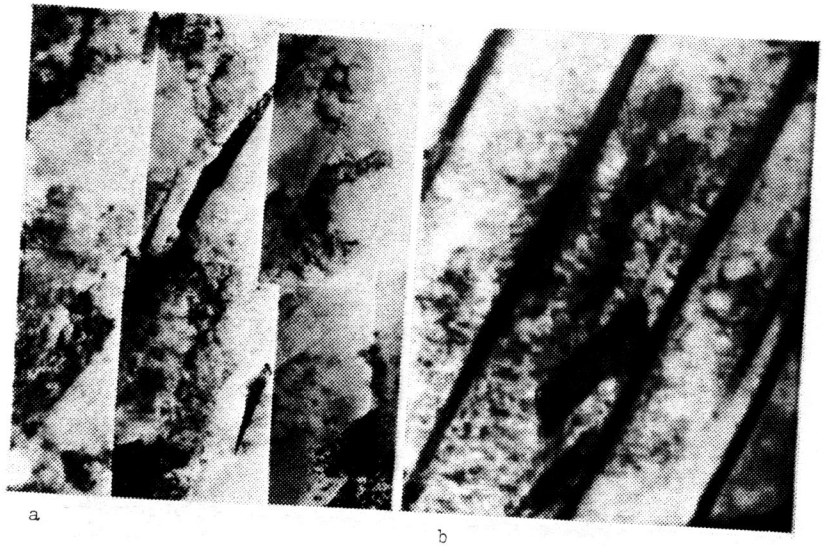

a b

Fig 3. Structure of Fe-0.6 % C steel fragments.
(a) ferrite, (b) pearlite. HVEM.

Fig 3 shows the structure of fragments of the Fe-0.6 % C steel. The plane of the foil is parallel to the cylinder axis and one radius in the cylinder. The ferritic area in fig 3a shows a structure characteristic of material that has been subjected to shock waves with a maximum pressure exceeding 130 kbars at which the body-centered cubic ferrite transforms to hexagonal ε-phase at ambient temperatures (Loree et al 1966). When the pressure decreases below 130 kbars again, a reverse transformation back to ferrite takes place, and areas in mutual twin relation (shear plates) are formed in this new ferrite. Fig 3b shows a shear plate which has been created in the ferrite volume between two cementite lamellae in a pearlite colony. Qualitatively, the same features were observed in thin foils from fragments of all the materials studied. A limitation of this investigation so far has been that only thin foils from the central portion of the cylinder wall have been obtainable.

2. SEM investigation

The general features of the fracture surfaces of both radial and shear type are qualitatively identical for Fe-0.6, -1.2 and 1.4 % C, and are illustrated in the sequence of photomicrographs in figure 4, which are all from an Fe-0.6 % C fragment. Close to the outer surface, the radial surface is completely built up of brittle transcrystalline cleavage facets (fig 4a), and this fracture type is dominating over the whole radial surface except in the vicinity of the shear surface, as can be seen in fig 4a-d. However, small "islands" of dimpled structure can be found as in

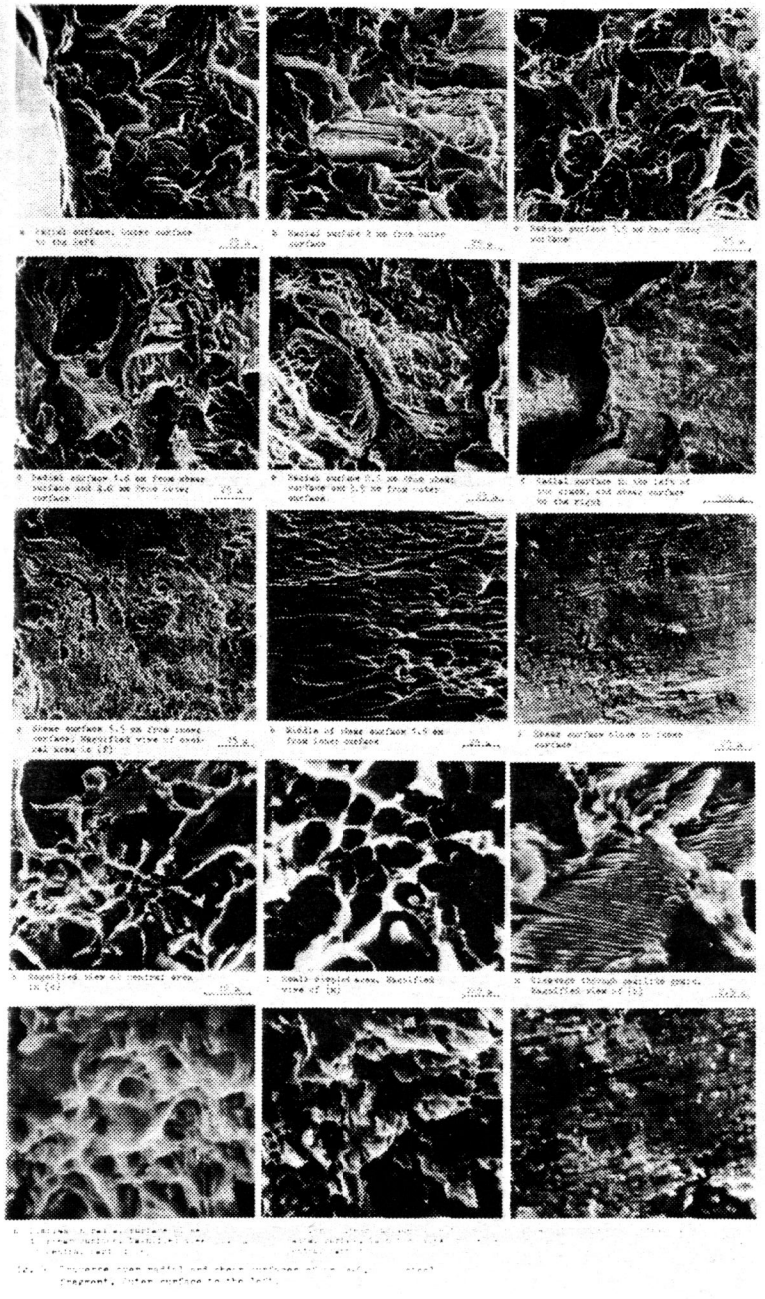

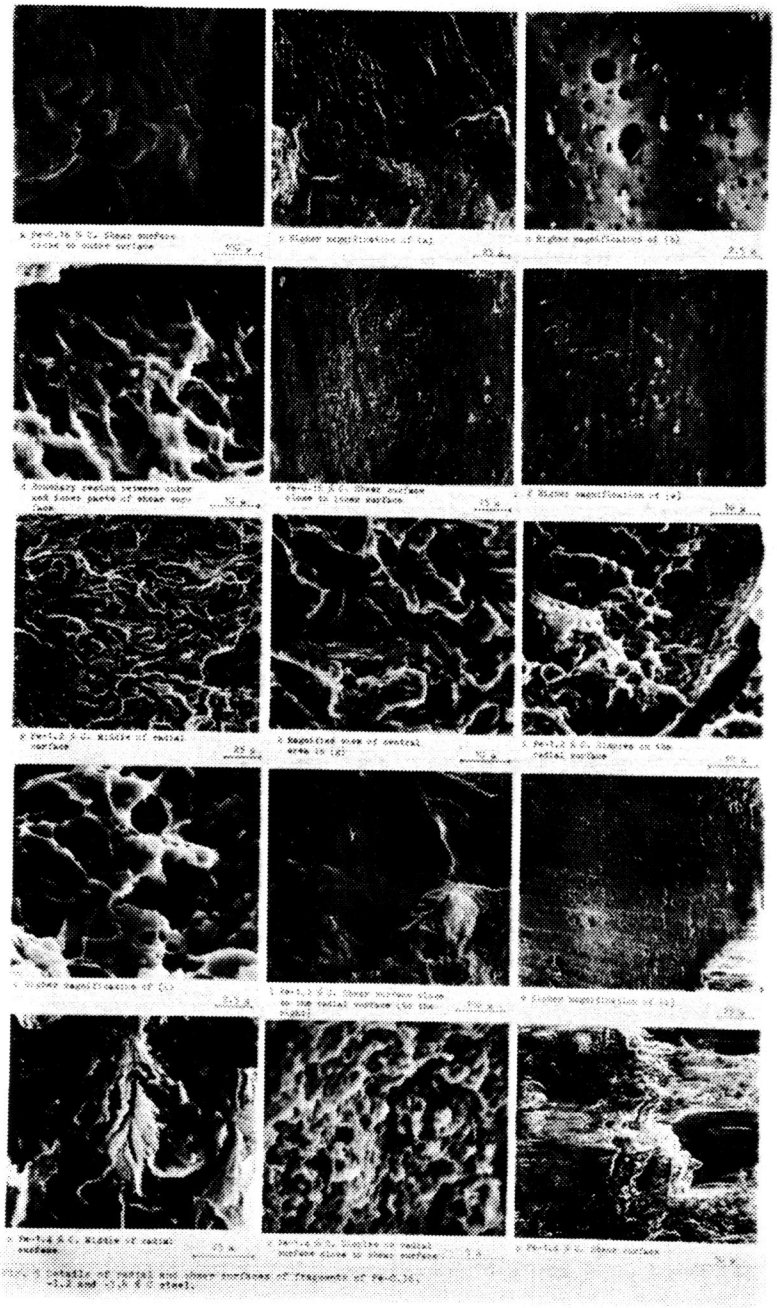

fig 4k, l. Fig 4m shows brittle cleavage through a pearlite grain. Close to the shear surface (0.3 mm, fig 4e, n) the fracture type is more ductile, as evidenced by the dimpled appearance of this part of the radial surface. The boarder between the radial and shear surfaces is shown at low magnification in fig 4f. As in this picture, cracks are very often observed in this region. The shear surface part in this picture is shown at higher magnifications in fig 4g and o. It can be seen that the shear surface too shows a dimpled appearance close to the boarder between radial and shear surface. At larger distances from this boarder, the structure gradually becomes more featureless (fig 4h) and close to the inner cylinder surface a faint streaking perpendicular to the edge is the most prominent feature (fig 4i, p).

It is interesting to compare these findings with those of Beetle et al (1971) who obtained very similar results for an Fe-.51 % C -.81 % Si steel (table 1).

In fig 5a-f the shear surface of an Fe-0.16 % C fragment is shown. As was inferred with reference to fig 1b, these fragments have no radial fracture surfaces. However, the features of the shear surface are distinctly different close to the outer and inner cylinder surfaces respectively. Thus fig 5a-c were obtained from a region close to the outer surface, and 5e, f close to the inner surface. There also exists a boundary region between the two types of surface which is sometimes quite pronounced (fig 5d), and cracks are often observed in this region.

In fig 5g-k details from the radial surface of an Fe-1.2 % C fragment is shown, and as in the case of Fe-0.6 % C fragments the dominating fracture type is transgranular cleavage. However, some evidence was obtained for micro-crack formation in grain boundaries, as in fig 5h. This was also observed on Fe-1.4 % C fragments (stereo pair of fig 6), and is consistent with the observation of grain boundary cementite films which lead to local embrittlement. Small dimpled areas are also observed in the vicinity of the shear surface as in fig 5i, k (compare fig 4l and 5k).

The dimpled regions on the radial surface close to the shear surface in the Fe-1.4 % C steel (fig 5o) seemed to be smaller in this material than in the Fe-0.6 % C steel.

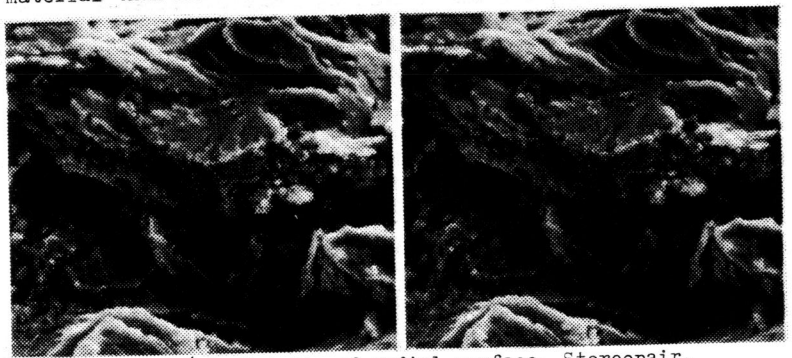

Fig 6. Fe-1.4 % C. Details of radial surface. Stereopair.

DISCUSSION

The characteristic shape of fragments of the three high-carbon materials with a radial surface adjacent to the outer cylinder surface and a shear surface adjacent to the inner surface can be qualitatively understood from a consideration of the stress state in the cylinder wall during the first expansion after the detonation of the high explosive. Due to the extremely rapid outward acceleration of the cylinder wall, inertial forces are set up which give rise to a compressive hoop stress in the cylinder wall, counteracting the tensile hoop stress due to the increase of the diameter of the cylinder. In a region extending outwards from the inner surface of the cylinder where the inertial forces are strongest, the resultant hoop stress is compressive. Therefore, according to a theory due to Hoggatt and Recht (1968), the fracture process is initiated with nucleation of radial cracks close to the outer cylinder surface where a state of tensile hoop stress is first developed. The inward propagation of these cracks is stopped in the region where compressive hoop stress exists; here the expansion of the cylinder proceeds entirely by plastic deformation. Due to the heat generated at the rapid dislocation motion, plastic instabilities develop and the deformation is concentrated to certain planes of maximum shear stress. The regions surrounding these shear planes are accordingly weakened, and when the region of compressive hoop stress gradually shrinks as the expansion of the cylinder proceeds, the cracks tend to propagate towards the inner surface along these weakened planes, and the shear surfaces are created.

In the case of Fe-0.16 % C steel, the material is so ductile that no radial cracks are nucleated, and the shear surfaces extend through the whole wall thickness.

The above model is substantiated by two observations in the present study. In fig 1a it can be seen that in the region from the inner surface and approximately one third through the wall thickness, which is roughly the region through which the shear surfaces extend, the grains are elongated in a direction parallel to the inner surface, whereas the grains in the rest of the wall are equiaxed. This shows that the radial cracks relieved the stresses in the material between the cracks before much plastic deformation had occurred, and thus before the fragments separated from each other across the shear surfaces.

It is further evident from a comparison of the shear surfaces of fragments of the four materials (see e.g. figs 4a, p and 5e, f, m) that the appearance of these surfaces is essentially identical, independent of the composition and microstructure of the material. This indicates that the mechanism responsible for the creation of the shear surfaces is extremely insensitive to these material parameters.

It is also clear that the radial surfaces of fragments of the three high-carbon steels show very great similarities. This implies that the fracture process is qualitatively the same in all these materials, and the observed differences in fragmentation number are entirely due to variations in the abundance of cracks.

Banks (1969) has pointed out that an increase in the number of radial cracks, which run in a zig-zag way more or less parallel to the cylinder axis, leads to an increase in the number of fragments not only by dividing the circumference of the cylinder into smaller strips, but also by increasing the chance that the radial cracks run together, so that the strips are broken up along their length. This process was termed longitudinal break-up. Banks (1969) studied the fragmentation of comparatively thin-walled cylinders (0.09 in) and concluded that the extent of longitudinal break-up was the main factor controlling the fragmentation number. In our case, with a wall thickness of 9 mm, the fragmentation of the shell case involves one more step, which might be termed internal break-up, in which the pieces created at the longitudinal break-up are disintegrated into the final fragments, the great majority of which carry only a small portion of the outer or inner surface, or none. It seems equally reasonable to assume that a high density of cracks promotes also this last step in the fragmentation process.

REFERENCES

Banks, E E, J Appl Phys 40, 437 (1969).

Beetle, J C, Rinnovatore, J V and Corrie, J D, Proc 4th Ann Symposium on Scanning Electron Microscopy, Chicago (1971).

Hoggatt, C R and Recht, R F, J Appl Phys 39, 1856 (1968).

Hörner, S and Kemgren, E, FOA 2 Report C 2196-44 (1967).

Johnsson, Å, FOA 2 Report C 2529-D4 (1972)

Loree, T R, Fowler, C M, Zukas, E G and Minshall, F S, J Appl Phys 37, 318 (1966).